Computional Cost of Nonrigid Registration Algorithms Based on Fluid Dynamics

Gert Wollny* and Frithjof Kruggel

Abstract—**Though fluid dynamics offer a good approach to nonrigid registration and give accurate results, even with large-scale deformations, its application is still very time consuming. We introduce and discuss different approaches to solve the core problem of nonrigid registration, the partial differential equation of fluid dynamics. We focus on the solvers, their computional costs and the accuracy of registration. Numerical experiments show that relaxation is currently the best approach, especially when reducing the cost/iteration by focusing the updates on deformation spots.**

Index Terms—**Computional cost, fluid dynamics, medical images, registration.**

I. Introduction

NONRIGID image registration is a problem in medical computer vision that has many applications. For instance, nonrigid registration can be used to detect changes in magnetic resonance (MR) time series images, arising when pathological processes (e.g., tumor growth, scarification, and atrophies) are monitored by a temporal series of MR examinations. Another application is nonrigid image-atlas registration that is used to locate brain-structures in the images.

Registration is achieved by applying one transformation to one image (which we call the study image), in order to match another (reference) image with respect to a given cost function. In practice, these transformations must accommodate both very complex and large deformations.

Early approaches of nonrigid registration, first introduced by Baiscy *et al.* [1], [2], later by Evans *et al.* [3], Miller *et al.* [4], and Christensen *et al.* [5], were all based on linear elasticity. As linear elasticity restricts the registration to globally smooth and therefore to locally small deformations, these methods fail to achieve very complex and/or large deformations. In an extension to their initial work, Christensen *et al.* [6] described a registration approach in which a viscous fluid model was used to control the deformation. In particular, the study image is modeled as a viscous fluid which is able to flow so as to match the reference. In this model internal forces disappear gradually, due to the attenuation in viscous fluids. This way, the desired deformation can be fully achieved, even if large-scale deformations are required. Other approaches to nonrigid registration are discussed in the literature (cf. e.g., [7]–[9]), but will not be considered in this paper.

The original implementation of fluid dynamics based registration, based on *successive over-relaxation* (SOR), is demanding with respect to computional cost and is thus time consuming. Bro-Nielsen *et al.* [10] proposed a further algorithm, based on *convolution filters* (CONV). They suggest that its performance results in a speedup of at least an order of magnitude.

In this paper, we will compare the original algorithm of Christensen [6], to the convolution based algorithm of Bro-Nielsen [10], and to an alternative, which is based on the *minimum residual algorithm* (MINRES), in terms of speed, memory usage, and registration accuracy. We will study optimization by employing an adaptive update scheme, which focuses on regions with significant deformations. Finally, we will demonstrate that it is possible to achieve good registration results for high resolution MR imaging (MRI) brain image data sets, in a reasonable amount of time on workstation class computers.

II. Registration Based on Fluid Dynamics

If not indicated otherwise, all numbers, vectors, matrices, and functions considered in this paper are real. Vectors are denoted as bold lower case characters, such as, $\mathbf{x}$, and $\mathbf{v}$, matrices appear as bold face upper case letters.

An image I is defined as a mapping $I\colon \Omega \to V$, with $\Omega := [0, 1]^3 \subset \mathbb{R}^3$ being the image domain and $V \subset \mathbb{R}$ being the (intensity-) range. The ordered pair $(\mathbf{x}, I(\mathbf{x})) \in \Omega \times V$ of a coordinate, and its corresponding intensity value is called a voxel (volume element). In the following $R\colon \Omega \to V$ denotes the reference and $S\colon \Omega \to V$ the study image.

The transformation $T\colon \Omega \to \Omega$ of an image I is a mapping of the image domain to itself, and Γ is the set of all such transformations. Following Christensen *et al.* [6], we use an *Eulerian reference frame* to describe a transformation T. Here, voxels of the deforming image are tracked by their position. Given a vector field $\mathbf{u}$, and a voxel originating at $\mathbf{x}$, at time $t_0 := 0$. With $\mathbf{u}(\mathbf{x}, t)$ being the displacement of this voxel at time t, its new location will be $\mathbf{x} - \mathbf{u}(\mathbf{x}, t)$. Hence, transformation T is defined as $T(\mathbf{x}, t) := \mathbf{x} - \mathbf{u}(\mathbf{x}, t)$. The concatenation of two transformations T_1 and T_2 with the displacement fields $\mathbf{u}_1$ and $\mathbf{u}_2$ is given by

$$T_1 \circ T_2 := \mathbf{x} - \mathbf{u}_1(\mathbf{x} - \mathbf{u}_2(\mathbf{x})) - \mathbf{u}_2(\mathbf{x}). \tag{1}$$

Additionally, the velocity field in an Eulerian reference frame is determined by [6]

$$\mathbf{v}(\mathbf{x}, t) = \frac{\partial \mathbf{u}(\mathbf{x}, t)}{\partial t} + \nabla \mathbf{u}(\mathbf{x}, t)\mathbf{v}(\mathbf{x}, t) \tag{2}$$

Manuscript received September 18, 2000; revised May 2, 2002. The Associate Editor responsible for coordinating the review of this paper and recommending its publication was R. Leahy. *Asterisk indicates corresponding author.*

*G. Wollny is with the Max-Plank-Institute of Cognitive Neuroscience, 04103 Leipzig, Germany (e-mail: wollny@cns.mpg.de).

F. Kruggel is with the Max-Plank-Institute of Cognitive Neuroscience, 04103 Leipzig, Germany.

Digital Object Identifier 10.1109/TMI.2002.803113

with the latter term $\nabla \mathbf{u}(\mathbf{x}, t)\mathbf{v}(\mathbf{x}, t)$ accounting for the kinematic nonlinearity of the voxels.

The purpose of registration is to find a transformation $T_{\min}$, which minimizes a given cost function $F_c(T, S, R)$ in conjunction with some energy normalization (or smoothness measure) $E(T)$

$$T_{\min} := \arg\min_{T \in \Gamma}(F_c(T, S, R) + \kappa E(T)) \tag{3}$$

with κ being a Lagrangian multiplier to balance registration accuracy and transformation smoothness.

Solving this minimization problem (3), can be done by finding the zero point of its first-order derivative

$$\kappa \frac{\partial}{\partial T} E(T) = -\frac{\partial}{\partial T} F(T, S, R). \tag{4}$$

As we study synthetically generated transformations only, the study image as well as the reference image will have the same intensity distribution. Hence, we use the simplest case of a similarity measure,[1] the so-called *identity relationship* [15], which yields the sum of squared intensity differences as a cost function

$$F_c(T, S, R) := \tfrac{1}{2} \int_{\Omega} [R(\mathbf{x}) - S(T(\mathbf{x}))]^2 \, d\mathbf{x}. \tag{5}$$

Its first-order derivative is then used as the force $\mathbf{f}$ to drive the registration

$$\begin{aligned} \mathbf{f}(\mathbf{x}, T(\mathbf{x}, t)) &:= \frac{\partial}{\partial T} F(T, S, R)\Big|_{\mathbf{x}} \\ &= [S(T(\mathbf{x}, t)) - R(\mathbf{x})] \nabla S|_{T(\mathbf{x}, t)}. \end{aligned} \tag{6}$$

Using fluid dynamics as the energy regularization, and with $\kappa := 0$ (4) finally reads

$$(\mu \nabla^2 + (\mu + \lambda)\nabla(\nabla \cdot))\mathbf{v}(\mathbf{x}, t) = -\mathbf{f}(\mathbf{x}, \mathbf{u}(\mathbf{x}, t)) \tag{7}$$

with μ and λ being Lamé's elasticity constants [16]. The term $\mu \nabla^2 + (\mu + \lambda)\nabla(\nabla \cdot)$ is the Navier–Stokes operator, modified to account for nonmass-conserving deformations [17].

Solving the registration problem is done iteratively over a time step of Δt. In each step, (7) is solved for a constant time to estimate the current velocity field $\mathbf{v}$, which is then used to update the displacement field $\mathbf{u}$ by a time integration step derived from (2)

$$\mathbf{u}(\mathbf{x}, t_{i+1}) := \mathbf{u}(\mathbf{x}, t_i) + \Delta t[\mathbf{v}(\mathbf{x}, t_i) - \nabla \mathbf{u}(\mathbf{x}, t_i)\mathbf{v}(\mathbf{x}, t_i)]. \tag{8}$$

To solve the registration problem, the continuous image domain Ω is discretized by using a grid constant $g > 1$, $g \in \mathbb{N}$

$$\Omega \to \widehat{\Omega} := \left\{ \frac{1}{g-1} \begin{pmatrix} i \\ j \\ k \end{pmatrix} \middle| \, i, j, k = 0, 1, \ldots, g-1 \right\}. \tag{9}$$

[1]For a detailed discussion of similarity measures, see [11]–[14]

With $n := g^3$, the discretization of a vector field $\mathbf{x}$ on the domain $\widehat{\Omega} \subset \mathbb{R}^3$ corresponds to a n-dimensional vector $[\mathbf{x}_0, \mathbf{x}_1, \ldots, \mathbf{x}_{n-1}]^T$. Given $m := i + jg + kg^2$ $(i, j, k) \in \widehat{\Omega}$, the mth component $\mathbf{x}_m$ is also denoted as $\mathbf{x}_{i,j,k}$.

Since we work on a discretized image domain, the transformation T is not preserving topology, *per se*. Therefore, we have to keep the minimal value of the Jacobian of transformation T [18]

$$J(T) := \min_{\mathbf{x} \in \Omega} \det(\mathbf{I} - \nabla \mathbf{u}(\mathbf{x}, t)) \tag{10}$$

from falling below a certain threshold. Christensen *et al.* [6] achieve this by re-gridding: Every time $J(T)$ drops below the heuristic value 0.5, the global deformation T is updated $T := T \circ T_t$ by using the current transformation $T_t := \mathbf{x} - \mathbf{u}(\mathbf{x}, t)$, and a new template $\hat{S}$ is generated by applying the current transformation $\hat{S} := S(T)$. The displacement field $\mathbf{u}$ and time t are set zero, and for further registration the new template $\hat{S}$ is used.

To avoid local minima and to speed up computation, a coarse-to-fine multi-resolution scheme can be employed voluntarily: We start with a coarse discretization of the image domain Ω, introduced by a low grid constant g. If registration is achieved at a certain grid level, the grid constant will be increased. The obtained transformation is tri-linearly interpolated on the higher resolution, thus assuming that the minimal value of the transformation's Jacobian is still positive. The multi-resolution iteration is stopped when the grind constant g is as large as the finite resolution of the input images. For implementation details of the registration algorithm, please refer to the software we made available online under the terms of the GNU public license [19].

To compare the results of registration approaches, finally a measure for registration accuracy has to be introduced. Since the synthetical transformation, used to deform the images, usually will not minimize the energy regularization term, comparing this transformation to the obtained registration transformation is not an option. Instead, we propose an accuracy measure based on the relative value of the cost function: With identity mapping $T_0(\mathbf{x}) := \mathbf{x} \, \forall \, \mathbf{x} \in \Omega$, the accuracy of registration achieved by the transformation $T(\mathbf{x})$: $\Omega \to \Omega$ is defined as

$$A_{\text{reg}}(T) := \frac{F_c(T_0, S, R)}{F_c(T, S, R)}. \tag{11}$$

Given a perfect registration, the accuracy becomes infinite. For interpolation of the image date during registration introduces errors in the image data, we do not expect infinite registration accuracy in our experiments.

III. Approaches for Solving the Linear PDE

The time consuming step of this registration algorithm, and therefore its core problem, is the solution of PDE (7) for a constant time and force. We will now discuss different approaches for its solution on the discretized coordinate domain $\widehat{\Omega}$, namely A): successive over-relaxation; B): successive over-relaxation with adaptive update; C): the minimal residual algorithm; and D): CONV. We will compare the approaches in terms of speed, memory usage, and accuracy of the resulting registration.

A. Successive Over-Relaxation (SOR)

Discretizing (7), using finite differences [20], yields a linear system

$$\mathbf{A}\mathbf{v} = \mathbf{f}, \qquad \mathbf{A} \in \mathbb{R}^{3n\times 3n},\ \mathbf{v},\ \mathbf{f} \in \mathbb{R}^{3n}. \tag{12}$$

One method to solve (12) is *successive over-relaxation* (SOR) [20]–[23]. Splitting $A = (a_{r,s}) \in \mathbb{R}^{3n\times 3n}$ into a diagonal matrix $\mathbf{A}_d$, a lower left matrix $\mathbf{A}_l$, and an upper right one $\mathbf{A}_r$

$$\mathbf{A} = \mathbf{A}_d + \mathbf{A}_l + \mathbf{A}_r \tag{13}$$

we obtain the iteration rule of SOR, with the iteration index l and the over-relaxation factor ω

$$\mathbf{v}^{(l+1)} := \mathbf{v}^{(l)} + \omega\mathbf{A}_d^{-1}\left(\mathbf{f} - \mathbf{A}_l\mathbf{v}^{(l+1)} - (\mathbf{I} + \mathbf{A}_r)\,\mathbf{v}^{(l)}\right). \tag{14}$$

In each iteration, the component $\mathbf{v}_m$ of vector field $\mathbf{v}$ is updated with a residual

$$\mathbf{r}_m^{(l+1)} := \frac{\omega}{a_{mm}} \cdot \left(\mathbf{f}_m - \mathbf{v}_m^l - \sum_{j=1}^{m-1} a_{m,j}\mathbf{v}_j^{(l+1)} - \sum_{j=m+1}^{n} a_{m,j}\mathbf{v}_j^{(l)}\right). \tag{15}$$

Note, that in the term $\sum_{j=1}^{m-1} a_{m,j}\mathbf{v}_j^{(l+1)}$ $j < m$, i.e., to evaluate $\mathbf{r}_m^{(l+1)}$, already updated elements of $\mathbf{v}$ are used.

The sparse structure of $\mathbf{A}$ yields that one update of the discretized velocity field $\mathbf{v}$ needs an order of $66n$ floating point operations ($O(66n)$ FLOPs) [19]. The update scheme does not require additional memory cells for the iteration process.

B. Successive Over-Relaxation With Adaptive Update

Nonrigid registration is usually preceded by rigid registration. Thus, we only expect differences between the images in certain regions of interest. Since we do a coarse-to-fine multi-resolution processing, large differences are roughly registered at coarser levels, yet. Hence, large regions of the images may have little (if any) influence on the solution of PDE (7).

By deriving the residuum $\mathbf{r}_{i,j,k} = \mathbf{r}_m$ (15), in each iteration $\mathbf{v}_{i,j,k}$ depends only on the 19 values with indexes $\beta \in \Im$

$$\Im := \left\{ \begin{pmatrix} i \\ j \\ k \end{pmatrix}, \begin{pmatrix} i\pm 1 \\ j \\ k \end{pmatrix}, \begin{pmatrix} i \\ j\pm 1 \\ k \end{pmatrix}, \begin{pmatrix} i \\ j \\ k\pm 1 \end{pmatrix}, \begin{pmatrix} i\pm 1 \\ j\pm 1 \\ k \end{pmatrix}, \begin{pmatrix} i \\ j\pm 1 \\ k\pm 1 \end{pmatrix}, \begin{pmatrix} i\pm 1 \\ j \\ k\pm 1 \end{pmatrix} \right\}. \tag{16}$$

Therefore, it makes sense to update $\mathbf{v}_{i,j,k}$ only if at least one residuum $\|\mathbf{r}_{\beta\in\Im}\|$ is larger then a threshold value $\hat{r}$ evaluated in the preceding iteration step

$$\hat{r} := \begin{cases} 0, & m = 1 \\ \overline{r}^{(m)} \cdot \dfrac{\overline{r}^{(m)}}{\overline{r}^{(m-1)}} \cdot \dfrac{1}{m^2}, & \text{otherwise} \end{cases} \tag{17}$$

with

$$\overline{r} := \frac{1}{X \cdot Y \cdot Z}\sqrt{\sum \|\mathbf{r}_{i,j,k}\|^2}. \tag{18}$$

To obtain all residues $\mathbf{r}_{i,j,k}$ initially, this threshold $\hat{r}$ is set to zero during the first iteration. Later on, the threshold is set to the average over the square norms $\overline{r}$ of the residual vectors combined with a term which involves the evolution of the respective residuum and another term to decrease the threshold in subsequent iterations, generally. With an increasing number of iterations, the solution search space thus increases and converges to the search space of the original SOR. Hence, if SOR is convergent, then SOR with adaptive update (SORA) will also converge. This update scheme (SORA) can also be seen as a variant of the Gauss–Southwell-Relaxation [24].

The number of operations, needed for one update of the velocity field, depends on the input data, but is well below the $O(66n)$ FLOPs that are needed for the unmodified SOR. Additional storage $O(n)$ is required for residues and update markers.

C. The Minimum Residual Algorithm (MINRES)

The solution of the linear system (12) can also be regarded as the minimum of

$$\Phi(\mathbf{v}) := \tfrac{1}{2}\left(\mathbf{A}\mathbf{v} - \mathbf{f}\right)^2. \tag{19}$$

If $\mathbf{A}$ is a symmetric matrix, though not necessarily a positive definite one, the MINRES[2] [21], as a variant of the conjugate gradient method, can be employed to solve this minimization problem.

In the linear system (12), the diagonal elements of $\mathbf{A}$ are $a_{i,i} = 1$, thus the system can be considered as treated with a Jacobi pre-conditioner. For the simple structure, a multiplication with $\mathbf{A}$ is achieved with only $O(51n)$ FLOPs [19]. Hence, solving (12) by using MINRES seems feasible. In summary, this algorithm requires $O(117n)$ FLOPs/iteration [19]. No storage for $\mathbf{A}$ is required, but the algorithm requires $O(n)$ storage cells for temporary vectors. Employing an adaptive update, similar to the one given for SORA, would break the search strategy of MINRES, which depends on orthogonal search directions. Thus, an adaptive update was not considered.

D. Convolution Filters

Bro-Nielsen *et al.* [10] suggested the usage of CONV for solving (7). A linear operator comprising the form of (7) is given as

$$\Lambda := \mu\nabla^2 + (\mu + \lambda)\nabla(\nabla\cdot). \tag{20}$$

With a filter width parameter d, the filter components $\Theta \in \mathbb{R}^{3\times 3}$, as given by Bro-Nielsen [25], and $\mathbf{y}_{r,s,t} = (r/d,\ s/d,\ t/d)^T | r,\ s,\ t \in [-d,\ d] \cap \mathbb{Z}$, the solution of PDE

[2]The usage of the standard conjugated gradient method (CG) is discouraged; without any boundary conditions, $\mathbf{A}$ is singular and thus not positive definite. Even with boundary conditions specified, for large n $\mathbf{A}$ becomes ill conditioned, which will lead to an instable operation of CG.

TABLE I
COMPUTIONAL COST TO SOLVE (7)

SOR iteration	SORAU iteration	MINRES iteration	$CONV_3$	$CONV_5$	$CONV_7$	$CONV_9$
$O(66n)$	$\leq O(66n)$	$O(117n)$	$O(486n)$	$O(2250n)$	$O(6174n)$	$O(13122n)$

TABLE II
RATIO OF COST OF ITERATIVE METHODS WITH RESPECT TO CONV

	$CONV_3$	$CONV_5$	$CONV_7$	$CONV_9$
SOR	8	35	94	199
MINRES	5	20	53	113

(7) at $\mathbf{x} \in \widehat{\Omega}$ can be calculated by convoluting the impulse response of operator Λ with the input force $\mathbf{f}$

$$\mathbf{v}(\mathbf{x}) = \sum_{r,s,t=-d}^{d} \Theta(\mathbf{y}_{r,s,t}) \cdot \mathbf{f}(\mathbf{x} - \mathbf{y}_{r,s,t}). \tag{21}$$

The filter components $\Theta \in \mathbb{R}^{3\times 3}$ can be pre-calculated. For each location (r, s, t) in (21) a product with a 3×3 matrix and the sum of two 3-D vectors have to be calculated. The computional cost for solving (7) on the discretized grid $\hat{\Omega}$ is $O(18(2d+1)^3 n)$ FLOPs, therefore. Additional storage space is only needed for the filter components; it can be neglected, because the filter width is small compared to the image size. A given filter width restricts the maximum length of the deformation during a transformation step in the registration algorithm. For a filter width smaller than the largest image dimension, it is not possible to obtain an accurate solution of PDE (7). Thus, a multi-resolution approach for solving the registration problem is mandatory to accommodate large deformations [10].

We now compare approaches A–D with respect to the respective computional costs, as obtained in (Table I). MINRES needs nearly twice as many FLOPs/iteration as SOR does. Since CG-based methods are known for their fast convergence, MINRES may perform better. The cost of CONV increases very quickly with a growing filter width.

To get a first impression of the performance ratio between CONV and iterative methods, we additionally summarize the number of iterations, with which the theoretical computional cost of these methods exceed the ones of the convolution based solver (Table II). These numbers indicate, that using CONV with large filter sizes does not offer an advantage compared to iterative solvers, if the number of iterations can somehow be restricted with these methods. On the other hand, we have to consider which filter sizes are sufficient to solve (7) with an adequate precision to achieve a good registration.

IV. EXPERIMENTS AND RESULTS

Convergence properties of solvers for systems of linear equations, such as SOR, SORA and MINRES, are well known from literature (e.g., [20]). Nevertheless, we first ran a test to determine the performance of the iteration methods alone, i.e., outside the context of the registration problem, since the actual convergence properties are also problem specific. Discrete random force fields $\mathbf{f}$ on a grid of $128 \times 128 \times 128$ voxels were generated, and (7) was solved. Every time the relative residuum of the solution dropped below a certain threshold during the iteration,

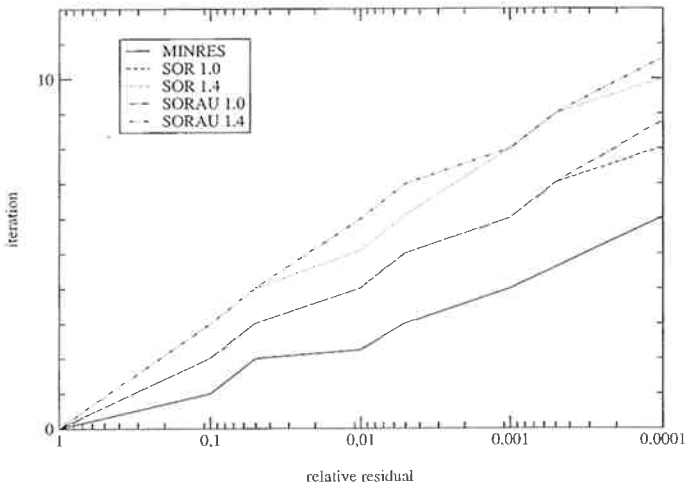

(a)

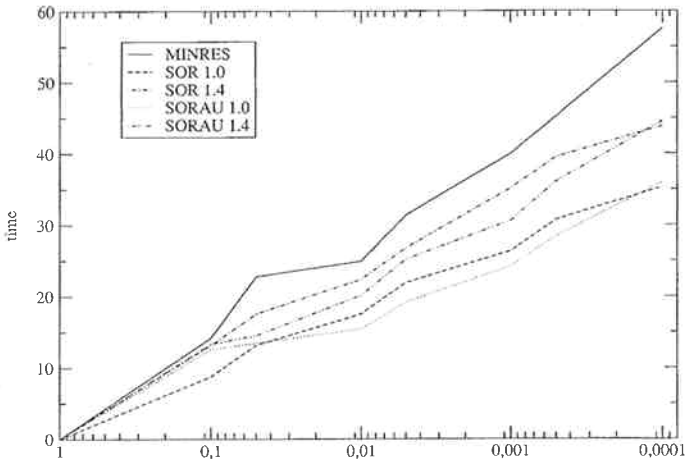

(b)

Fig. 1. (a) MINRES shows the best convergence properties in term of iteration count. (b) However, in terms of execution time, SOR and SORA perform best, because their cost/iteration is well below that of MINRES.

time and number of iterations were measured. If matrix $\mathbf{A}$ is a symmetric, positive definite, tridiagonal, or block-wise tridiagonal matrix, the theoretically optimal relaxation factor ω can be approximated by

$$\omega = \frac{2}{1 + \sqrt{1 - \lambda^2}} \tag{22}$$

with λ being the *spectral radius* of $\mathbf{A}_d^{-1}(\mathbf{A}_l + \mathbf{A}_r)$ [20]. Since it is difficult to calculate the spectral radius, we used relaxation factors of 0.8, 1.0, 1.4, and 1.8. A dynamic adaption scheme, known as Chebyshev acceleration [20], was also examined, but did not offer any improvement.

Fig. 1(a) shows[3] that the minimal residual method (MINRES) requires least iterations to achieve a given relative residuum. In

[3]Relaxation factors of 0.8 and 1.8 did not yield superior results over factors 1.0 and 1.4 and were omitted from figures.

TABLE III
TIME AND ACCURACY FOR SOLUTION OF PDE (7) USING CONV

	3		5		7		9	
time (s)	23.9	(0.1)	111.4	(0.3)	312.5	(0.5)	723.4	(1.0)
$\frac{res(v_{sol})}{res(v=0)}$	0.44	(0.01)	0.42	(0.04)	0.40	(0.07)	0.39	(0.13)

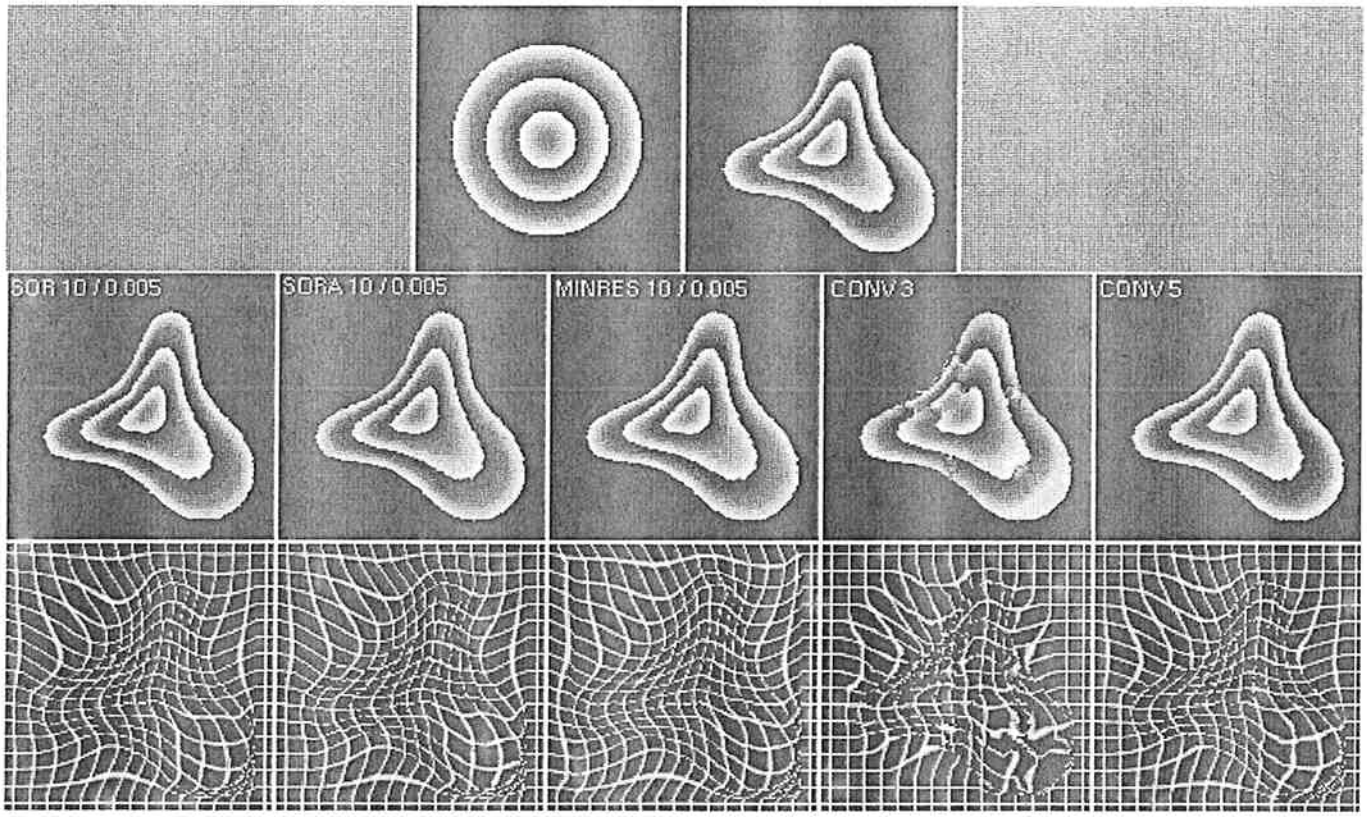

Fig. 2. Registration of a synthetic study (top-left) and an example reference (top-right). Results are shown in the middle row, and the obtained deformations in the lower row. Iterative methods were applied using a limit of ten iterations and $\varepsilon = 0.01$. Note the registration error when using a small filter width ($CONV_3$).

terms of computation time, (using a 450 MHz Pentium II based workstation), however, successive over-relaxation was faster [see Fig. 1(b)].

In the generated fields, forces are distributed evenly over the domain, therefore the adaptive update showed only a slight advantage. We expect better results on realistic data, because forces will typically be localized. An over-relaxation factor of 1.0 achieved best results for the relaxation based methods, and it was used in the following registration experiments. On the basis of this experiment, we expect SOR or SORA to perform better than MINRES.

The same test was run with CONV. Especially by using small filter widths, results for the solution of PDE (7), were not satisfactory (Table III). This conforms with the statement that CONV does not yield a proper solution of (7), if the filter width is much below the image dimensions. Filters of higher order were not tested, since their high computional costs do not offer an advantage compared to the iterative methods.

For our second experiment, the performance of the different methods was tested in the framework of the registration algorithm by using synthetic images of size $64 \times 64 \times 64$ (see also Fig. 2). Twenty reference images were generated, deforming the study with a smooth random deformation field, and the study was registered to these references. We choose $\mu = \lambda = 1.0$ and the multi-resolution start grid constant $g = 16$.

Results in Table IV demonstrate, that it is not necessary to solve (7) with a high accuracy. A limit of ten iterations only, yields a registration quality nearly as good as any higher number of iterations. For CONV, a minimum filter width of five is necessary to achieve results which are similar to those of the other methods (see Table III and Fig. 2). The bad registration results for a filter width of 3, again show that a small filter is not sufficient to solve (7) with an adequate accuracy. The number of iterations in the iterative methods can be reduced significantly, i.e., it is not necessary to evaluate the velocity field $\mathbf{v}$ accurately from the deforming force $\mathbf{f}$ in each iteration step. Thus the computational cost of CONV is similar to those methods, and any speed advantage vanishes. Only with a filter width of three CONV offers an advantage, in terms of speed but not in terms of accuracy. These results correspond to the ratio of computational costs, as compiled in Table II.

Now, we were interested in testing how algorithms scale on the image resolution, using the optimal parameters as determined in the preceding experiment. For the iteration based

TABLE IV
REGISTRATION OF SYNTHETIC IMAGES (ITERATIVE METHODS)

	MINRES				SOR				SORA			
max iterations \ ϵ	0.01		0.005		0.01		0.005		0.01		0.005	
10	9.2	(1.2)	10.2	(2.0)	4.7	(1.0)	4.7	(1.3)	**3.5**	(0.7)	**3.5**	(0.7)
	10.4	(1.2)	10.2	(1.4)	10.6	(1.3)	10.5	(1.3)	10.3	(1.3)	10.3	(1.3)
20	13.4	(2.8)	19.8	(6.3)	8.0	(1.6)	9.3	(1.8)	**5.7**	(1.0)	**5.8**	(1.0)
	10.6	(0.9)	10.9	(1.1)	10.2	(1.1)	10.4	(1.1)	10.0	(0.9)	10.2	(1.1)
80	**26.0**	(4.5)	**31.5**	(15.3)	53.5	(17.4)	55.3	(16.9)	51.8	(10.7)	44.2	(10.3)
	10.5	(0.9)	9.1	(2.5)	10.8	(0.8)	10.6	(0.9)	11.0	(0.7)	10.7	(0.7)

TABLE V
REGISTRATION OF SYNTHETIC IMAGES (CONVOLUTION FILTERS)

	$CONV_3$		$CONV_5$		$CONV_7$		$CONV_9$	
time (min)	4.4	(0.5)	10.6	(2.5)	28.5	(8.0)	60.3	(13.7)
A_{reg}	5.0	(1.7)	10.9	(1.9)	11.2	(1.5)	11.3	(1.1)

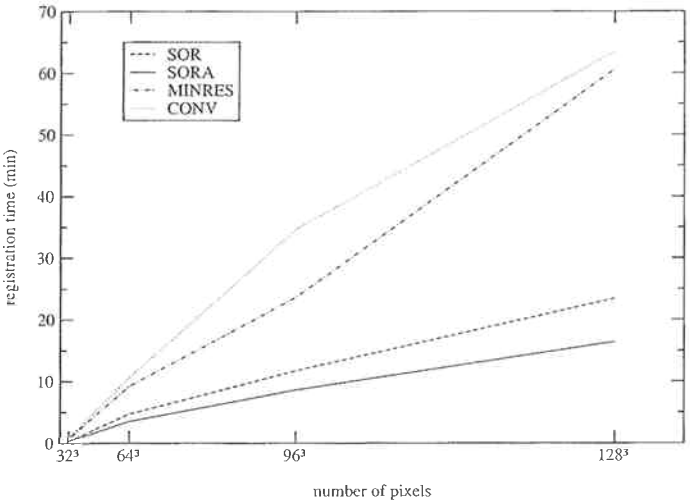

Fig. 3. Scaling of the execution times with image size: All methods show a subproportional time increase with respect to images of size 64 × 64 × 64. SORA scales best.

methods, we set the maximum number of iterations to 10, or stopped if the relative residuum dropped below 0.01. Convolution filters were applied with a filter width of 5. Although methods for solving (7) need $O(n)$ FLOPs, the time needed to achieve registration of synthetic images increased at a lower rate than the number of voxels (see Fig. 3).

As another conclusion, SOR and SORA scale better than MINRES and CONV. The super-scalar speed increase for small resolutions (i.e., 32 × 32 × 32) is a consequence of caching [26]. SORA proved to be the fastest method.

Finally, we explored the performance of registering high-resolution medical image data. Acceptable results of the registration of pairs of 250 × 250 × 192 MR image of the head were achieved in approximately 3 hours.

V. CONCLUSION

We compared two iterative methods *successive over-relaxation* (SOR), and the *minimal residuum algorithm* (MINRES), and a direct approach CONV, as methods for the solution of the core problem of nonrigid registration, based on fluid dynamics. In terms of computional costs, we found that MINRES required fewer iterations to solve (7) with a given accuracy, but SOR required less memory cells as well as less time to achieve the same result, and is thus considered superior. Numerical experiments on synthetic data demonstrated the possibility of restricting the numbers of iterations drastically, without a significant loss of accuracy of the registration result. With this optimization, SOR outperformed CONV in terms of speed while the registration accuracy maintains. Furthermore, we were able to speedup SOR by introducing an adaptive update scheme (SORA). In summary, SORA proved to be the best approach to solve (7).

Although our implementation is neither fully optimized for workstation architectures nor parallelized we were able to obtain results for MRI volumetric data of high resolution, in approximately three hours of computation time. By optimizing our implementation (e.g., by improving the use of the memory cache hierarchies of the processor and by introducing parallelization), a further speedup is expected.

ACKNOWLEDGMENT

The authors would like to thank M. Tittgemeyer and N. H. Busch for their helpful discussions, librarians G. Lewin and A. Hutt for providing the necessary literature, and a special acknowledgment is given to all the creators of free software, since they made extensive use of their work.

REFERENCES

[1] R. Bajcsy and S. Kovacic, "Multi-resolution elastic matching," *Comput. Vis., Graph. Image Processing*, vol. 1, no. 46, pp. 1–21, 1989.
[2] J. C. Gee, M. Reivich, and R. Bajcsy, "Elastically deforming atlas to match anatomical brain images," *J. Comput. Assist. Tomogr.*, no. 17, pp. 255–236, 1993.
[3] A. C. Evans, W. Dai, L. Collins, P. Neelin, and S. Marret, "Warping of a computerized 3-D atlas to match brain image volumes for quantitative neuroanatomical and functional analysis," in *Proc. SPIE Medical Imaging V*, vol. 1445, 1991, pp. 236–246.
[4] M. I. Miller, G. E. Christensen, Y. Amit, and U. Grenander, "Mathematical textbook of deformable neuroanatomies," in *Proc. Nat. Acad. Sci. USA 90*, 1993, pp. 11 944–11 948.
[5] G. E. Christensen, M. I. Miller, and M. Vannier, "A 3-D deformable magnetic resonance textbook based on elasticy," in *AAAI Spring Symp. Series: Applications of Computer Vision in Medical Image Processing*. Stanford, CA, Mar. 1994, pp. 153–156.
[6] G. E. Christensen, "Deformable shape models for neuroanatomy," D.Sc. dissertation, Server Inst. Technol., Washington Univ., Saint Louis, MO, 1994.
[7] O. Musse, F. Heitz, and J.-P. Armspach, "Topology preserving deformable image matching using constrained hierarchical parametric models," *IEEE Trans. Image Processing*, vol. 10, pp. 1087–1093, July 2001.

[8] K. Rohr, H. S. Stiehl, R. Sprengel, J. Buzug, T. M. Weese, and M. H. Kuhn, "Landmark-based elastic registration using approximating thin-plate splines," *IEEE Trans. Med. Imag.*, vol. 20, pp. 526–543, July 2001.

[9] J. P. Thirion, "Fast nonrigid matching of 3-D medical images," INRIA, Sophia-Antipolis, France, Tech. Rep., 1995.

[10] M. Bro-Nielsen and C. Gramkov, "Fast fluid registration of medical images," in *Lecture Notes in Computer Science*. Berlin, Germany: Springer-Verlag, Sept. 1996, vol. 1131, Visualization in Biomedical Computing (VBC'96), pp. 267–276.

[11] M. Holden, D. L. G. Hill, E. R. E. Denton, J. M. Jariosz, T. C. S. Cox, and D. J. Hawkes, "Voxel similarity measures for 3-D serial MR brain image registration," in *Lecture Notes in Computer Science*, A. Šámal Kuba and A. M. Todd-Pokropek, Eds. Berlin, Germany: Springer-Verlag, 1999, vol. 1613, Information Processing in Medical Imaging, pp. 472–477.

[12] A. Roche, G. Malandain, X. Pennec, and N. Ayache, "Multimodal image registration by maximization of the correlation ratio," INRIA, Sophia-Antipolis, France, Tech. Rep., 1998.

[13] C. Studholme, D. L. G. Hill, and D. J. Hawkes, "Multi-resolution voxel similarity measures for MR-PET registration," in *Proc. IPMI'95*, pp. 187–198.

[14] C. Studholme, D. J. Hawkes, and D. L. G. Hill, "An overlap invariant entropy measure of 3-D medical image alignment," *Pattern Recogn.*, vol. 32, no. 1, pp. 71–86, 1999.

[15] A. Roche, G. Malndain, N. Ayache, and S. Prima, "Toward a better comprehension of similarity measures used in medical image registration," in *Lecture Notes in Computer Science*. Berlin, Germany: Springer-Verlag, 1999, vol. 1679, Proc. MICCAI'99, pp. 555–566.

[16] L. A. Segel, *Mathematics Applied to Continuum Mechanics*, ser. Classics of Science and Mathematics. New York: Dover, 1987.

[17] G. E. Christensen, R. D. Rabbitt, and M. I. Miller, "Deformable templates using large deformation kinematics," *IEEE Trans. Med. Imag.*, vol. 5, pp. 1435–1447, Oct. 1996.

[18] P. G. Ciarlet, *Mathematical Elasticy*. Amsterdam, The Netherlands: North-Holland, 1993, vol. I, Three-Dimensional Elasticy.

[19] G. Wollny. (2002) Mia—A toolchain for medical image analysis. [Online]. Available: http://mia.sourceforge.net.

[20] W. H. Press, S. A. Teukolsky, W. T. Vetterling, and B. P. Flannery, *Numerical Recipes in C*, 2nd ed. New York: Cambridge Univ. Press, 1992.

[21] R. Barrett, M. Berry, T. F. Chan, J. Demmel, J. M. Donato, J. Dongarra, V. Eijkhout, R. Pozo, Ch. Romine, and H. Van der Vorst. (1993) Templates for the solution of linear systems: Building blocks from iterative methods. [Online]. Available: http://www.netlib.org/templates/templates.ps.

[22] G. Engeln-Müllges and F. Reutter, "Formelsammlung zur Numerischen Mathematik mit Turbo Pascal Programmen," Bibliographisches Institut & F. A. Brockhaus AG, Mannheim, Germany, 3. aufl. ed., 1991.

[23] C. C. Paige and M. A. Saunders, "Solution of sparse indefinit systems of linear equations," *SIAM J. Numer. Anal.*, vol. 12, no. 4, pp. 866–869, 1975.

[24] R. Southwell, *Relaxation Methods in Engineering Science—A Treatise in Approximate Computation*. Oxford, U.K.: Oxford Univ. Press, 1940.

[25] M. Bro-Nielsen, "Medical image registration and surgery simulation," Ph.D. dissertation, Tech. Univ. Denmark, Lyngby, Denmark, 1996.

[26] B. Greer and G. Henry. (1997) High-performance software on Intel pentium pro processors or micro-ops to teraflops. [Online]. Available: http://www.supercomp.org/sc97/program/TECH/GREER/INDEX.HTM.